An alternative approach to create N -substituted cyclic dipeptides

Ozgul Tezgel, Sylvie Servagent Noinville, Véronique Bennevault, Nicolas Illy, Philippe Guégan

▶ **To cite this version:**

Ozgul Tezgel, Sylvie Servagent Noinville, Véronique Bennevault, Nicolas Illy, Philippe Guégan. An alternative approach to create N -substituted cyclic dipeptides. Polymer Chemistry, 2019, 10 (6), pp.776-785. 10.1039/c8py01552j . hal-02188779

HAL Id: hal-02188779

https://hal.sorbonne-universite.fr/hal-02188779

Submitted on 18 Jul 2019

HAL is a multi-disciplinary open access archive for the deposit and dissemination of scientific research documents, whether they are published or not. The documents may come from teaching and research institutions in France or abroad, or from public or private research centers.

L'archive ouverte pluridisciplinaire **HAL**, est destinée au dépôt et à la diffusion de documents scientifiques de niveau recherche, publiés ou non, émanant des établissements d'enseignement et de recherche français ou étrangers, des laboratoires publics ou privés.

An alternative approach to create *N*-substituted cyclic dipeptides†

Özgül Tezgel,[a] Sylvie Noinville,[b] Véronique Bennevault,[a,c] Nicolas Illy *[a] and Philippe Guégan *[a]

N-Modified peptide backbones are promising peptidomimetics which offer several advantages in terms of improved biological activity and stability. They further allow the development of novel functional materials. However, the synthesis of *N*-substituted peptides is very challenging with the existing methods, particularly the synthesis of peptides with larger *N*-substituents. In this work, we are introducing a new method to create *N*-polyether substituted cyclic dipeptides *via* anionic ring-opening polymerization (AROP). Four different cyclic dipeptides with different hydrophobic functional groups were selected to create *N*-substituted cyclic dipeptides. Backbone amides –*N**H**H*– were deprotonated with phosphazene bases to form nucleophilic initiators. Furthermore, the effect of different phosphazene bases (*t*BuP$_4$ and *t*BuP$_2$) and of the addition of a Lewis acid (i-Bu$_3$Al) was studied in detail towards creating *N*-polyether-cyclic dipeptides bearing either hydrophobic poly(butylene oxide) chains, or hydrophilic linear polyglycidol chains, thanks to the polymerization of 1,2-epoxybutane and the polymerization followed by the deprotection of *t*-butyl glycidyl ether monomers, respectively. Moreover, we have demonstrated the possibility of avoiding the isomerization of cyclic dipeptides during the synthesis of *N*-substituted analogues depending on the synthetic approach.

Introduction

In the last few decades, cyclic dipeptides, so-called 2,5-diketopiperazines (DKPs), have attracted significant attention due to their exceptional biological activity as antiviral,[1,2] antimicrobial[3,4] and anticancer[5,6] agents. Beyond their therapeutic properties, DKPs also have the ability to form supramolecular structures[7–9] which could find a wide range of applications, such as hydrogels,[10,11] nano-devices,[12] and sensors.[13] In addition, due to their structural rigidity, *N*-substituted DKPs are also used as rigid motifs on the polypeptide backbone to imitate protein secondary structures.[14] Moreover, in the field of peptide-based drugs, *N*-substituted peptides often demonstrated superior outcomes in terms of biological activity and stability.[15–17] Peptides with *N*-substitution could also offer the creation of a novel class of materials, for which *N*-substitution will potentially change the peptide conformation and induce new properties. For example, polypeptoids are one of the most popular classes of peptidomimetics which are basically short *N*-alkyl substituted glycine analogues with remarkable properties.[18–20] Indeed, the antimicrobial peptoid derivatives with long *N*-alkyl chains create lipophilic peptoids which are shown to be more selective against bacteria and fungi than their non-lipophilic analogues.[21] Other than functionalisation with peptoids, *N*-methylation is the most commonly used tool to improve the biological activity of peptide drugs.[15,16,22,23] However, there is also a limited number of studies reported for other *N*-substituted analogues, such as peptides with *N*-substituted short alkyl groups, *i.e.* *N*-ethyl,[24] *N*-butyl,[25] and *N*-guanidyl butyl.[26] More recently, Albericio and coworkers have reported the synthesis of *N*-oligoethylene glycol (*N*-OEG) substituted cyclic peptides: sansalvamide A with 3 repeat units of *N*-OEG[27] and cilengitide with different repeat units of *N*-OEG such as 2, 11 and 23.[28] The synthesis of cilengitide with *N*-OEG$_2$ and sansalvamide A with *N*-OEG$_3$ by solid-phase peptide synthesis in multiple steps was reported; however, peptides with longer *N*-OEG substitutions were very complicated to synthesize and were reported to require extensive purification steps.[28] In the current work, we are introducing anionic ring-opening polymerization (AROP) as a novel technique to create peptides with *N*-polyether derivatives in a one-step reaction without sophisticated purification steps. AROP is an effective method which is frequently used to synthesize

[a]*Sorbonne Université, CNRS, Institut Parisien de Chimie Moléculaire, Equipe Chimie des Polymères, 4 place Jussieu, F-75005 Paris, France. E-mail: nicolas.illy@sorbonne-universite.fr, philippe.guegan@sorbonne-universite.fr*
[b]*Sorbonne Université, CNRS, MONARIS, 4 place Jussieu, F-75005 Paris, France*
[c]*University of Evry, 91025 Evry, France*

†Electronic supplementary information (ESI) available: ^{1}H, ^{13}C, 2D-HSQC, and 2D-HMBC NMR spectra, SEC traces and MALDI-ToF spectra. An additional scheme of plausible configurations. See DOI: 10.1039/c8py01552j

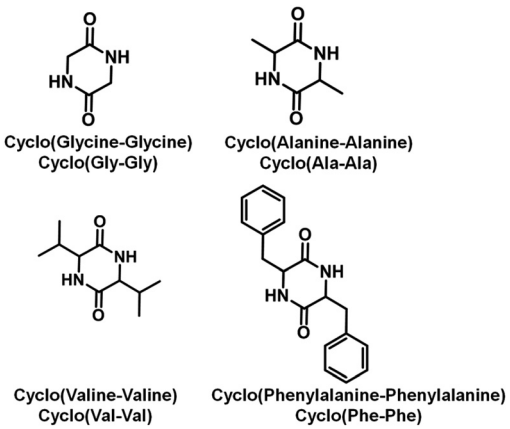

Fig. 1 Structures of di-functional symmetric DKPs.

various functional polymers readily applicable in the biomedical field.[29–31] Phosphazene superbases construct powerful catalytic systems for the polymerization of different heterocyclic rings through AROP as a result of their high basicity and poor nucleophilicity coming from their sterically hindered structure.[32,33] They could easily deprotonate protic precursors to create nucleophilic initiating sites for the polymerization of oxirane monomers. Recently, we have demonstrated the polymerization of 1,2-epoxybutane with a secondary carbamate[34] and a secondary amide.[35]

In this study, we selected di-functional symmetric DKPs (Fig. 1) with different hydrophobic functional groups, such as glycine, alanine, valine and phenylalanine, as model cyclic peptides due to their structural simplicity and interesting behaviors.[36] The backbone *–NH–* of symmetric DKPs was deprotonated by phosphazene bases to create nucleophilic initiating species for the polymerization of 1,2-epoxybutane and of a commercially available protected analogue of glycidol, *t*-butyl glycidyl ether (*t*BuGE). The reaction conditions were optimized with 1,2-epoxybutane. First, the use of phosphazene base mixtures with different tBuP$_2$/tBuP$_4$ ratios has been investigated. Then the influence of a Lewis acid addition has been considered. The positive impacts of using a less basic phosphazene base,[32] tBuP$_2$, and the presence of a Lewis acid, triisobutyl aluminum (i-Bu$_3$Al), have been demonstrated. Both methods yielded *N*-substituted-DKPs with expected structures. However, we have observed by NMR and FT-IR the ring conformation differences of DKPs under different conditions of synthesis. Eventually, the optimized conditions were extended to the polymerization of *t*BuGE, a protected version of glycidol.

Results and discussion

We have investigated the possibility of creating *N*-substituted DKPs using oxirane monomers *via* AROP in the presence of phosphazene bases. We attempted to synthesize *N*-substituted analogues of four different symmetric cyclic dipeptides with varying hydrophobic functional groups (Fig. 1).

Synthesis of *N*-PBO-Cyclo(Ala–Ala) using phosphazene bases (tBuP$_4$ and tBuP$_2$)

In the first part of this work, we have used Cyclo(Ala–Ala) (Scheme 1) as an initiator precursor for the polymerization of 1,2-epoxybutane in the presence of phosphazene bases (Table 1). Cyclo(Ala–Ala) was chosen in the first place due to the presence of an alanine sequence which is considered as a neutral, chemically inert peptide residue.[37] Initially, 1,2-epoxybutane was polymerized with Cyclo(Ala–Ala)/tBuP$_4$ as the initiator system at a ratio of 1 : 1 and 1 : 2 at 25 °C (Table 1, P1-1 and P1-2) to evaluate whether tBuP$_4$ works under stoichiometric conditions to deprotonate the backbone amide *–NH–* or not. In both cases, ^{1}H NMR analysis indicated the disappearance of *–NH–* protons, meaning 100% functionalization of both backbone amide *–NH*s. The MALDI ToF analysis of the polymerization carried out in the presence of 1 eq. of tBuP$_4$ (Table 1, P1-1) shows one major population corresponding to the expected polymer structure (Scheme 1A) cationized with the Na$^+$ cation (Fig. 3b). The MALDI-ToF analysis also indicates the presence of an additional minor unidentified population. A higher amount of tBuP$_4$ (2 eq., Table 1, P1-2) resulted in the increase of the undesired population (Fig. 3a). ^{1}H NMR and ^{13}C NMR and ATR-FTIR analyses (P1-1 and P1-2, Fig. 2a, b and 4a) clearly display the presence of ester bonds on the polymers. A macromolecular structure in agreement with these spectral analyses and corresponding to a nucleophilic attack on the DKP ring is postulated and shown in Scheme 1B. The intensity of ester peaks was increased by increasing the amount of tBuP$_4$, in both the NMR and ATR-FTIR spectra (P1-1 and P1-2, Fig. 2a, b and 4a). The coexistence of polymer structures A and B in P1-2 was also confirmed by 2D-NMR (2D-HSQC-NMR, Fig. S1† and 2D-HMBC-NMR, Fig. S2†). As a conclusion, *N*-substitution has been proved to be possible for the reactions performed with both 1 eq. and 2 eq. of tBuP$_4$. However, undesired nucleophilic attack on the DKP ring also occurred and the frequency of this side-reaction increased with the amount of tBuP$_4$. To eliminate the undesired side reactions, we have decided to decrease the amount of tBuP$_4$ ($pK_{BH^+,\ MeCN}$ = 42.7) and eventually use a mixture of tBuP$_4$ and a less basic phosphazene base, tBuP$_2$ ($pK_{BH^+,\ MeCN}$ = 33.5). When we decreased the amount of tBuP$_4$ to 0.5 eq. and performed the polymerization at 40 °C, we reached 100% conversion within 72 h (P1-5, Table 1) with expected molar mass and

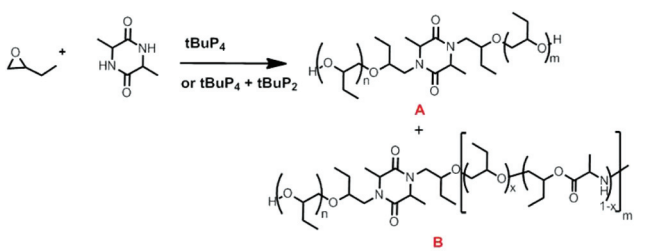

Scheme 1 Synthesis of *N*-PBO-Cyclo(Ala–Ala) using phosphazene bases.

Table 1 Polymerization of 1,2-epoxybutane using phosphazene bases and Cyclo(Ala–Ala) as the initiator system in THF at a monomer concentration of 2 mol L^{-1}

Run	tBuP$_4$[a]	tBuP$_2$[a]	X_n[a]	T (°C)	Time (h)	% conv.	$M_{n\ theo}$	$M_{n\ GPC}$	M_w/M_n
P1-1	1	—	30	25	19	100	2300	2500	1.16
P1-2	2	—	30	25	16	100	2300	2600	1.15
P1-3	0.50	0.50	30	25	96	82	1900	800	1.30
P1-4	0.50	0.50	30	40	18	100	2300	2500	1.13
P1-5	0.50	—	50	40	72	100	3700	3900	1.11
P1-6	0.25	0.75	30	40	66	0	—	—	—
P1-7	0.30	0.70	30	40	47	88	2000	1300	1.18
P1-8	0.25	1	30	40	72	100	2300	2700	1.12
P1-9	0.10	1	30	40	69	0	—	—	—

[a] Reactant equivalents compared to 1 equivalent of cyclo(Ala–Ala).

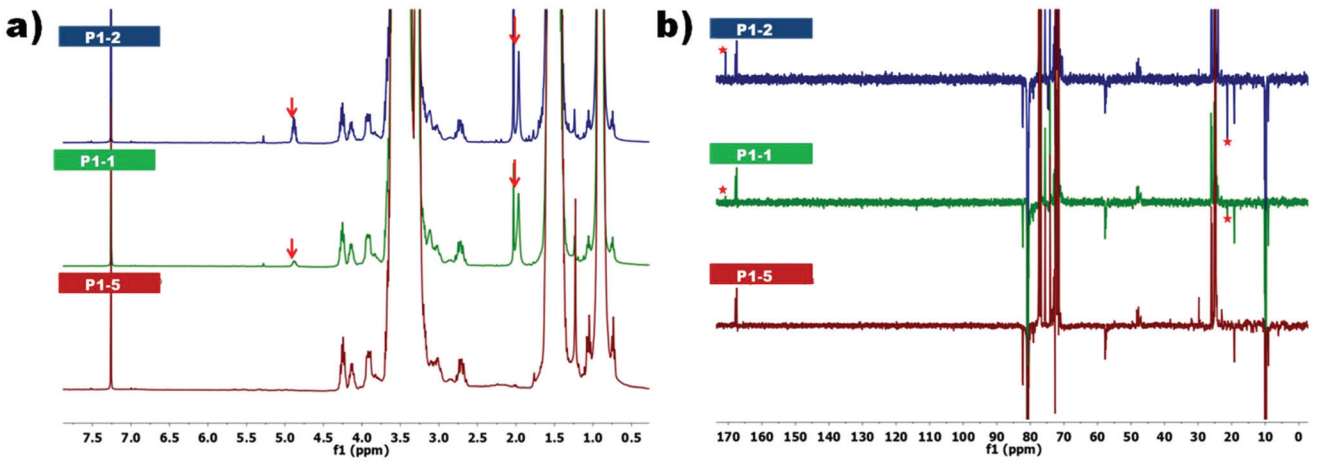

Fig. 2 NMR spectra showing the effect of the tBuP$_4$/Cyclo(Ala–Ala) ratio on the polymerization of 1,2-epoxybutane using Cyclo(Ala–Ala) and tBuP$_4$ as the initiating system. (a) ^{1}H NMR spectra in $CDCl_3$ comparing the tBuP$_4$/Cyclo(Ala–Ala) ratio of 2 (P1-2-blue), 1 (P1-1, green) and 0.5 (P1-5, red). The red arrows indicate the presence of side reactions. (b) ^{13}C NMR spectra in $CDCl_3$ comparing the tBuP$_4$/Cyclo(Ala–Ala) ratio of 2 (P1-2-blue), 1 (P1-1, green) and 0.5 (P1-5, red). The red stars show the presence of extra peaks occurring due to the side reactions.

narrow dispersity (P1-5, Table 1). In addition, ATR-FTIR (Fig. 4a) and ^{1}H and ^{13}C NMR analyses (Fig. 2, P1-5) demonstrated only the presence of an expected polymer structure (polymer **A**, Scheme 1). MALDI-ToF analysis shows only one population corresponding to the expected polymer A structure (Fig. 3c). We have tested the mixture of tBuP$_4$ and tBuP$_2$ for the polymerization of 1,2-epoxybutane by Cyclo(Ala–Ala)/tBuP$_4$/tBuP$_2$ at a ratio of 1 : 0.5 : 0.5. At 25 °C, the reaction did not go to completion over 96 h (P1-3, Table 1). At 40 °C (P1-4, Table 1), the polymerization achieved 100% conversion in 18 h with the desired molar mass (M_n) without the presence of ester peaks in the NMR spectra (Fig. S3 and S4†). These results suggest that 1 : 1 and higher ratios of Cyclo(Ala–Ala)/tBuP$_4$ decrease the stability of DKPs. The strong tBuP$_4$ super-base does not necessarily need to be introduced at a stoichiometric ratio for 100% functionalization of amides on the DKP backbone. Therefore, we investigated the use of the less basic phosphazene base tBuP$_2$ and only a catalytic amount of tBuP$_4$ to obtain the desired polymer structures (P1-6 to P1-9, Table 1). The ratio of 1 : 0.3 : 0.7 led to polymerization but the obtained M_n was smaller than the targeted one (P1-7, Table 1) and the polymerization of 1,2-epoxybutane by Cyclo(Ala–Ala)/tBuP$_4$/tBuP$_2$ at a ratio of 1 : 0.25 : 0.75 did not work at all (P1-6, Table 1).

Then, we increased the amount of tBuP$_2$ and kept the ratio of tBuP$_4$ at 0.25 eq. or below (P1-8 and P1-9, Table 1). The Cyclo(Ala–Ala)/tBuP$_4$/tBuP$_2$ ratio of 1/0.1/1 was not effective, on the other hand a 1/0.25/1 ratio of Cyclo(Ala–Ala)/tBuP$_4$/tBuP$_2$ worked with a good efficiency to yield the polymers with the desired *N*-PBO-Cyclo(Ala–Ala) structure (Fig. S5†) and targeted M_n with a narrow molar mass distribution (P1-8, Table 1). An absolute M_n value of 2600 g mol^{-1} was also determined by ^{1}H NMR and is in very good agreement with both theoretical and SEC values. It has been reported that 1,2-epoxybutane does not polymerize in the presence of the less basic phosphazene base tBuP$_2$.[38] Here, we demonstrated that 1,2-epoxybutane can be polymerized with tBuP$_2$ in the presence of a catalytic amount of tBuP$_4$ without undesired side reactions. All the techniques used for the characterization of *N*-PBO-Cyclo(Ala–Ala) indicated only the presence of the expected *N*-PBO-Cyclo(Ala–Ala)

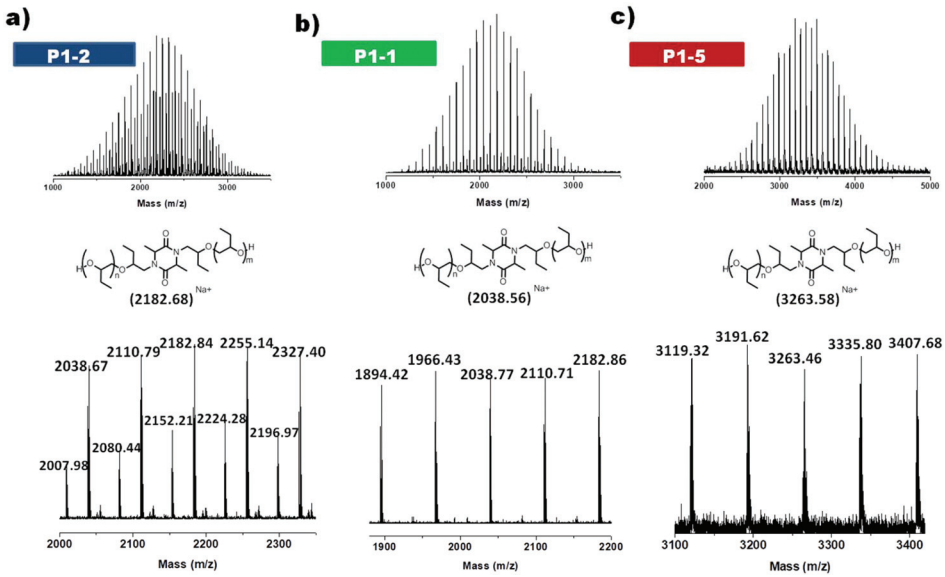

Fig. 3 MALDI-ToF analysis of polymers initiated by the tBuP$_4$/Cyclo(Ala–Ala) ratio of (a) 2, (b) 1 and (c) 0.5. Top spectra are collected in linear mode and the bottom ones are collected in reflectron mode. Major populations represent the structure of polymer **A**.

population with no evidence of free –*NH*– amide peaks, suggesting the growth of polymer chains at both DKP backbone amide functionalities (Scheme 1, polymer A).

Synthesis of *N*-PBO-Cyclo(Gly–Gly) using phosphazene bases (tBuP$_4$ and tBuP$_2$)

After the successful synthesis of *N*-PBO-Cyclo(Ala–Ala), we attempted to apply a similar approach to synthesize *N*-substituted analogues of Cyclo(Gly–Gly). The reactions with a Cyclo(Gly–Gly)/tBuP$_4$ ratio of 1 : 1 and 1 : 2 (P2-1 and P2-2, Table 2) yielded polymers with expected M_n. ATR-FTIR did not show a peak corresponding to ester formation confirming the integrity of the DKP ring. In addition, the MALDI-ToF analysis demonstrated a single polymer population corresponding to the *N*-PBO-Cyclo(Gly–Gly) (Fig. S6†). However, both the ^{13}C NMR and ATR-FTIR spectra of P2-2 indicate C=C double bond formation (Fig. S7†) which could be explained by the transfer reaction to the monomer at high concentrations of tBuP$_4$.[39]

^{13}C NMR analysis demonstrated multiple C=O amide peaks (P2-1, Fig. 5a) which could be explained by the formation of different isomers of the DKP ring following the addition of *N*-substituents.[40] This result could be attributed to the epimerization of cyclic dipeptides in basic solutions as already reported more than forty years ago.[41,42] A similar phenomenon is also observed for cyclic peptoids (*N*-substituted glycine analogues), for which each single C=O amide geometry displayed a single C=O amide peak[43] and in the presence of *cis*/*trans* isomers, multiple C=O amide peaks were observed.[43,44] Additionally, similar to the *N*-PBO-Cyclo (Ala–Ala) synthesis, a Cyclo(Gly–Gly)/tBuP$_4$ ratio of 1 : 0.5 yielded a polymer having the expected structure (Table 2, P2-5) without transfer reactions. ^{13}C NMR demonstrated a major single C=O amide peak (Fig. S8†) which indicates the presence of mainly a single isomer of the DKP ring. These results suggest that the use of tBuP$_4$ at 1 eq. and more favors the isomerization of the DKP ring and the occurrence of side reactions. Furthermore, a mixture of tBuP$_4$ and tBuP$_2$ was incorporated in the reaction mixture by varying the tBuP$_4$ percen-

Table 2 Polymerization of 1,2-epoxybutane using phosphazene bases and Cyclo(Gly–Gly) as the initiator system in THF at a monomer concentration of 2 mol L^{-1}

Run	tBuP$_4$[a]	tBuP$_2$[a]	X_n[a]	T (°C)	Time (h)	% conv.	$M_{n\ theo}$	$M_{n\ GPC}$	M_w/M_n
P2-1	1	—	30	25	19	92	2100	2400	1.22
P2-2	2	—	30	25	14	96	2300	2100	1.20
P2-3	0.5	0.5	30	25	120	0	—	—	—
P2-4	0.5	0.5	30	40	42	80	1800	1400	1.38
P2-5	0.5	—	30	40	72	100	2300	2700	1.13
P2-6	0.5	1	30	40	23	100	2300	2400	1.21
P2-7	0.25	1	40	40	69	100	3100	3700	1.10

[a] Reactant equivalents compared to 1 equivalent of Cyclo(Gly–Gly).

tage from 0.25 to 0.5 and the tBuP$_2$ percentage from 0.5 to 1 (P2-3, P2-4, P2-6 and P2-7, Table 2). The optimal conditions were determined as P2-7 (Fig. S9†), where the addition of tBuP$_2$ led to the formation of *N*-PBO-Cyclo(Gly–Gly) with mostly single ring configuration as confirmed by ^{13}C NMR (P2-7, Fig. 5a).

Synthesis of *N*-PBO-Cyclo(Val–Val) and *N*-PBO-Cyclo(Phe–Phe) using phosphazene bases (tBuP$_4$ and tBuP$_2$)

We were able to find the common reaction conditions for the synthesis of *N*-PBO-DKPs with Cyclo(Ala–Ala) and Cyclo(Gly–Gly). We would like to expand the validity of our method for more hydrophobic DKPs, Cyclo(Val–Val) and Cyclo(Phe–Phe).

The synthesis of *N*-substituted Cyclo(Val–Val) showed similar polymerization characteristics and side reactions to that of Cyclo(Ala–Ala). When the polymerization of 1,2-epoxybutane was carried out at a Cyclo(Val–Val)/tBuP$_4$ ratio of 1 : 1 (P3-1, Table 3), the MALDI-ToF spectrum displayed only single Poisson distribution corresponding to *N*-PBO-Cyclo(Val–Val) (Fig. S11a†). However, the ^{1}H NMR spectra show the presence of ester function due to the nucleophilic attack of growing polymer end chains on the DKP ring (Fig. S10†) which is also confirmed by ATR-FTIR analysis (Fig. 4b, red curve). The polymer obtained by the initiating system, Cyclo(Val–Val)/tBuP$_4$/tBuP$_2$, at a ratio of 1 : 0.5 : 0.5 also demonstrated the nucleophilic attack on the DKP ring at a lower degree (P3-2, Fig. S10†). Ester formations for Cyclo(Ala–Ala) and Cyclo(Val–Val) suggest that DKPs with aliphatic substitutions at the Cα position are more sensitive to nucleophilic attack during the synthesis in the presence of high concentrations of tBuP$_4$. When we applied the optimized conditions to the synthesis of *N*-PBO-Cyclo(Val–Val), *i.e.* 1 eq. of tBuP$_2$ with 0.25 eq. of tBuP$_4$ (P3-3, Table 3), ^{1}H-NMR and MALDI-ToF analyses did not show the presence of side reactions (P3-3, Fig. S10 and S11c†). At the same time, four different peaks are visible in the C=O amide region in the ^{13}C NMR spectrum (P3-3, Fig. 5b). The ATR-FTIR spectrum also demonstrates a peak at ~1700 cm^{-1} (Fig. 4b, green curve) which corresponds to the *cis* C=O amide stretching on the DKP ring[45] in addition to the C=O *trans* peak at ~1660 cm^{-1}. Thus, ATR-FTIR and ^{13}C NMR spectra demonstrate the presence of C=O amide peaks of both *cis* and *trans* isomers, meaning that *N*-substitution leads to the formation of isomers of the DKP rings (Scheme S1†). In the literature, DKPs have been reported to have four different configurations corresponding to two *cis* and two *trans* isomers[41] which could be easily characterized by ^{13}C NMR.[46] Therefore, the presence of four different peaks for C=O amide, **Cα** (presented as **2, 2′** in Fig. S12†), *N*-substituted –**C**H$_2$– (presented as **a′** in Fig. S12†) and Cα substituted –**C**H– (presented as **3** in Fig. S12†) in the ^{13}C NMR spectrum represents the four different configurations of the DKP ring (two *cis* and two *trans* isomers). The ratio of *cis*/*trans* isomers is known to be affected by the nature of the *N*-substituent in *N*-substituted peptides.[40] The synthesis of *N*-PBO-Cyclo(Phe–Phe) was more challenging. The optimized conditions (1 eq. of tBuP$_2$ with 0.25 eq. of tBuP$_4$) did not work at all (P3-6, Table 3). This lack of reactivity could pave the way to the selective functionalization of an asymmetric DKP containing only one phenylalanine residue; nevertheless, it is beyond the scope of the present work. In addition, the polymers obtained using 1 eq. of tBuP$_4$ at 25 °C

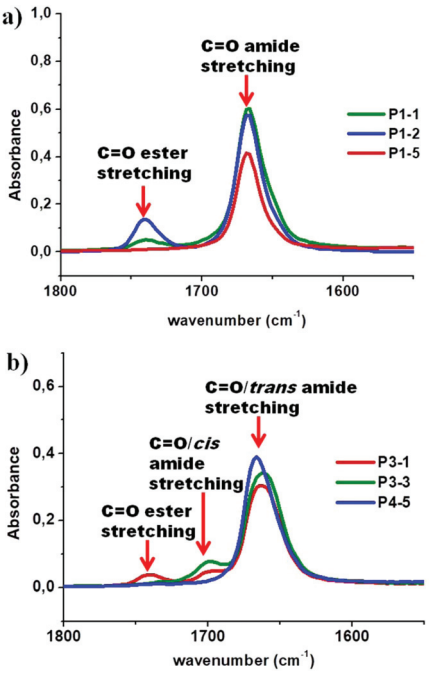

Fig. 4 ATR-FITR spectra of (a) *N*-PBO-Cyclo(Ala–Ala); P1-1 (green curve), P1-2 (blue curve), P1-5 (red curve) and (b) *N*-PBO-Cyclo(Val–Val); P3-1 (red curve), P3-3 (green curve), and P4-5 (blue curve).

Table 3 Polymerization of 1,2-epoxybutane using phosphazene bases and Cyclo(Val–Val) or Cyclo(Phe–Phe) as the initiator system in THF at a monomer concentration of 2 mol L^{-1}

Run	DKP	tBuP$_4$[a]	tBuP$_2$[a]	X_n[a]	T (°C)	Time (h)	Conv. (%)	$M_{n\ theo}$	$M_{n\ GPC}$	M_w/M_n
P3-1	Cyclo(Val–Val)	1	—	30	25	19	96	2300	2500	1.15
P3-2	Cyclo(Val–Val)	0.50	0.50	30	40	21	100	2400	2000	1.13
P3-3	Cyclo(Val–Val)	0.25	1	30	40	72	100	2400	2700	1.11
P3-4	Cyclo(Phe–Phe)	1	—	30	25	46	85	2100	1100	1.32
P3-5	Cyclo(Phe–Phe)	1	—	30	40	17	79	2000	900	1.48
P3-6	Cyclo(Phe–Phe)	0.25	1	30	40	70	30	—	—	—

[a] Reactant equivalents compared to 1 equivalent of DKP.

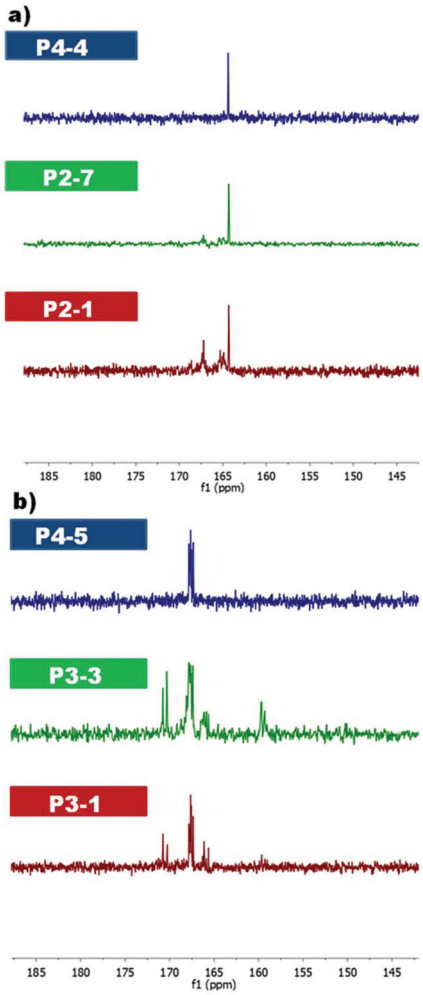

Fig. 5 ^{13}C NMR analysis of polymers (in $CDCl_3$) synthesized under different conditions. (a) Polymers initiated by (a) Cyclo(Gly–Gly); P2-1 (red curve), P2-7 (green curve), P4-4 (blue curve) and (b) Cyclo(Val–Val); P3-1 (red curve), P3-3 (green curve), and P4-5 (blue curve).

and 40 °C yielded lower molar masses than the expected ones and broad molar mass distributions (P3-4 and P3-5, Table 3). Besides, the MALDI-ToF spectra display two different populations (Fig. S13†); one corresponding to the expected structure of *N*-PBO-Cyclo(Phe–Phe), and the second one is unknown. Increasing the polymerization temperature from 25 °C (Table 3, P3-4) to 40 °C (Table 3, P3-5) led to an increase of the proportion of the unknown population and to a concomitant decrease of molar masses. ^{13}C NMR analysis also demonstrated the presence of multiple peaks indicating the DKP ring with multiple isomers and side reactions (Fig. S14†).

Synthesis of *N*-PBO-DKPs in the presence of *t*BuP$_4$ and a Lewis acid i-Bu$_3$Al

The synthesis of *N*-PBO-DKPs using the DKP/*t*BuP$_4$/*t*BuP$_2$ initiating system worked very well for Cyclo(Ala–Ala), Cyclo(Gly–Gly) and Cyclo(Val–Val). However, the synthesis of *N*-substituted Cyclo(Phe–Phe) was more challenging. Therefore, to overcome the challenges that we faced during the synthesis, we employed an alternative strategy. A Lewis acid, i-Bu$_3$Al, was incorporated in the reaction medium to control the reactivity of the active centers and to trigger monomer reactivity.[47] In the polymerization reactions with the addition of i-Bu$_3$Al, we kept the ratio of DKP/*t*BuP$_4$ constant at 1 : 1 and varied the amount of i-Bu$_3$Al from 2 eq. to 3 eq. As previously indicated, Cyclo(Ala–Ala) was used as a reference to test the reaction conditions (P4-1 and P4-2, Table 4). With 3 eq. of i-Bu$_3$Al (P4-1, Table 4), M_n was higher than the targeted value with a broad dispersity. An absolute M_n value of 4500 g mol^{-1} was also determined by ^1H NMR, which confirmed the value obtained by SEC. The polymerization control was better in the presence of 2 eq. of i-Bu$_3$Al (P4-2, Table 4). M_n was closer to the theoretical value (2700 *vs.* 2100 g mol^{-1}) with narrower dispersity. The characterization of *N*-PBO-Cyclo(Ala–Ala) which was synthesized in the presence of i-Bu$_3$Al did not show any difference compared to the one synthesized by the first approach. Furthermore, in the case of Cyclo(Gly–Gly), the polymerizations were performed in the presence of 2 eq. and 2.5 eq. of i-Bu$_3$Al (P4-3 and P4-4, Table 4). Polymer P4-3 which was synthesized in the presence of 2 eq. of i-Bu$_3$Al has a slightly broad distribution and ^{13}C-NMR analysis shows a main C=O peak with traces of other C=O peaks corresponding to isomeric structures (Fig. S15†). P4-4 that was synthesized in the presence of 2.5 eq. of i-Bu$_3$Al has a narrow molar mass distribution (P4-4, Table 4). Furthermore, ^{13}C-NMR analysis shows only one single peak in the amide-carbonyl region (P4-4, Fig. 5a), demonstrating the single isomer of the DKP ring. Therefore, using an optimized amount of

Table 4 Polymerization of 1,2-epoxybutane using phosphazene base i-Bu$_3$Al and DKPs as the initiating system in MeTHF at a monomer concentration of 2 mol L^{-1} at 25 °C

Run	DKP	*t*BuP$_4$[a]	i-Bu$_3$Al[a]	X_n	Time (h)	% conv.	$M_{n\ theo}$	$M_{n\ GPC}$	M_w/M_n
P4-1	Cyclo(Ala–Ala)	1	3	30	3	100	2300	4000	1.65
P4-2	Cyclo(Ala–Ala)	1	2	30	16	86	2100	2700	1.35
P4-3	Cyclo(Gly–Gly)	1	2	30	15	95	2300	3000	1.37
P4-4	Cyclo(Gly–Gly)	1	2.5	30	23	100	2300	4000	1.22
P4-5	Cyclo(Val–Val)	1	2	30	20	100	2400	3400	1.25
P4-6	Cyclo(Phe–Phe)	1	2	30	20	93	2300	3200	1.29
P4-7	Cyclo(Phe–Phe)	1	2.5	30	19	100	2500	3200	1.28

[a] Reactant equivalents compared to 1 equivalent of DKP.

i-Bu_3Al in the reaction medium helps us to eliminate the isomerization of the DKP ring, but a slight increase in the amount of i-Bu_3Al increases the difference between the targeted and obtained M_n (P4-3 *vs.* P4-4, Table 4).

N-PBO-Cyclo(Val–Val) synthesis in the presence of 2 eq. of i-Bu_3Al yielded a controlled polymerization with a narrow dispersity (P4-5, Table 4). Compared to the reactions without i-Bu_3Al, *cis* amide C═O peaks disappeared in the ^{13}C-NMR (Fig. 5b) and ATR-FTIR spectra (Fig. 4b). Moreover, there are also single peaks observed at the ring level (peaks **2** and **3**, Fig. S16b†) and two peaks observed for *N*-substituted –CH_2– on the polymer instead of four different peaks (peak **a′**, Fig. S16b†). These observations confirm that the synthesis of *N*-PBO-Cyclo(Val–Val) in the presence of 2 eq. of i-Bu_3Al led to the formation of *N*-substituted DKP with a single configuration. This could be explained by the stabilization of the active centers by i-Bu_3Al and their reduced basicity.

Lastly, *N*-PBO-Cyclo(Phe–Phe) synthesis was also performed in the presence of 2 eq. and 2.5 eq. of i-Bu_3Al (P4-6 and P4-7, Table 4). In both cases, we successfully obtained *N*-PBO-Cyclo (Phe–Phe) which was confirmed by NMR and MALDI-ToF analysis (P4-6, Fig. S17† and P4-7, Fig. 6). The polymerization kinetics and the control over the polymerization were better in the presence of 2.5 eq. of i-Bu_3Al compared to 2 eq. (P4-6 and P4-7, Table 4). Moreover, ^{13}C NMR analysis demonstrated the presence of a single isomer type of Cyclo(Phe–Phe) (Fig. 6c).

Synthesis of *N*-P*t*BuGE-DKPs. In this section, we demonstrated the synthesis of *N*-polyether-DKP analogues having a water soluble *N*-substituent using a commercially available protected version of the water soluble monomer glycidol, *t*-butyl glycidyl ether (*t*BuGE). Cyclo(Ala–Ala) and Cyclo(Gly–Gly) were successfully modified to create *N*-substituted analogues by two different strategies described above without side reactions.

N-Poly(*t*-butyl glycidyl ether) (*N*-P*t*BuGE) substituted DKPs were synthesized in the presence of 1 eq. of $tBuP_2$ and 0.25 eq. of $tBuP_4$ (P5-1 and P5-2, Table 5). Both polymers P5-1 and P5-2 have a very narrow mass distribution. However, the molar mass of P5-1 obtained by GPC was larger than the targeted value. MALDI-ToF characterization confirmed the expected polymer structures (P5-1, Fig. S18 and P5-2, Fig. S19†). Furthermore, the polymerization of *t*BuGE was also carried out in the presence of i-Bu_3Al. Initially, for the synthesis of *N*-P*t*BuGE-Cyclo(Ala–Ala), we have tested two different ratios of i-Bu_3Al (P5-3 and P5-4, Table 5). Between the two reactions, 2.75 eq. of i-Bu_3Al yielded a better control over the polymerization (P5-4, Table 5). Therefore, *N*-P*t*BuGE-Cyclo(Gly–Gly) was also synthesized using the same conditions (P5-5, Table 5). MALDI-ToF analysis of polymers P5-4 and P5-5 confirmed the

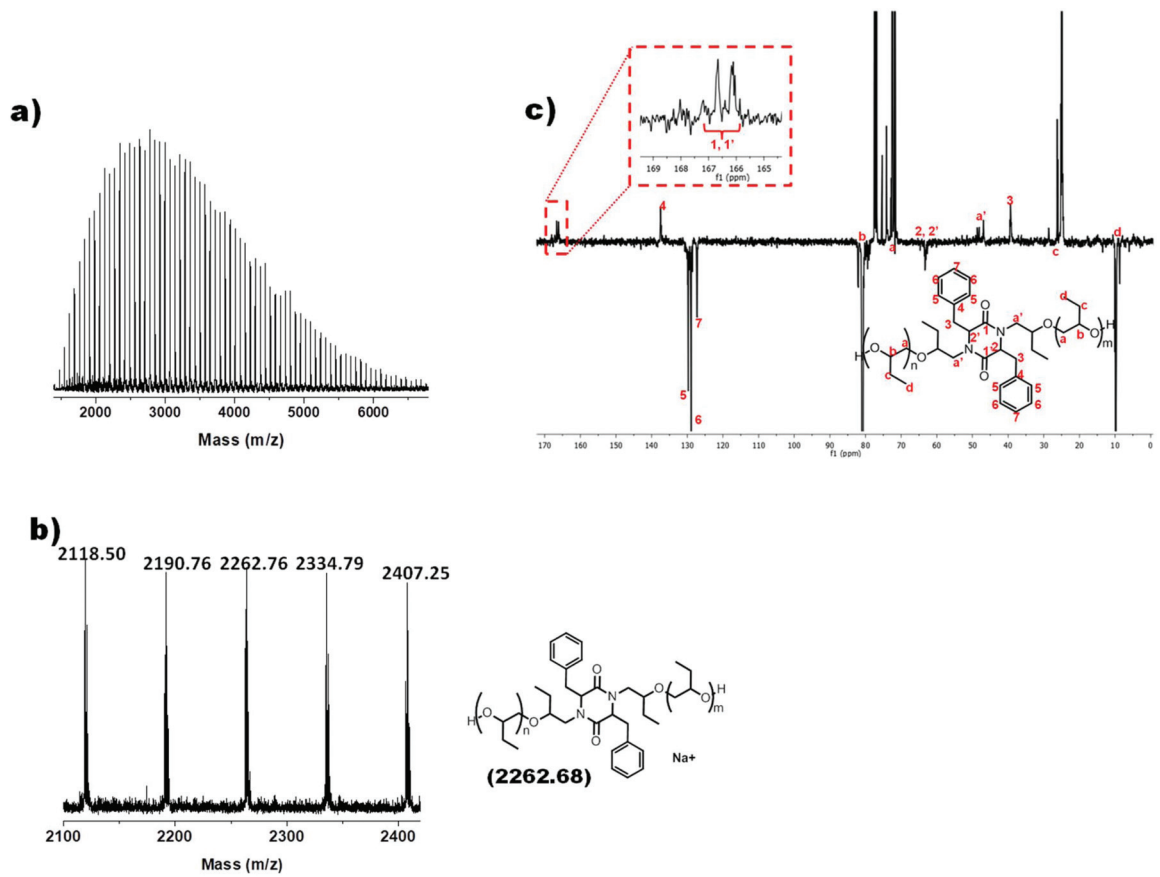

Fig. 6 MALDI-ToF and ^{13}C NMR analysis of P4-7. (a) MALDI-ToF spectrum of P4-7 in linear mode. (b) MALDI-ToF spectrum of P4-7 in reflectron mode. (c) ^{13}C NMR analysis of P4-7 in $CDCl_3$ at 50 °C.

Table 5 Synthesis of *N*-P*t*BuGE-DKPs under different conditions at a monomer concentration of 2 mol L^{-1}

Run	DKP	$tBuP_4$[a]	$tBuP_2$[a]	i-Bu_3Al[a]	*T* (°C)	Time (h)	% conv.	$M_{n\ theo}$	$M_{n\ GPC}$	M_w/M_n
P5-1[b]	Cyclo(Ala–Ala)	0.25	1	—	40	96	100	4000	5200	1.12
P5-2[b]	Cyclo(Gly–Gly)	0.25	1	—	40	96	100	4000	4400	1.10
P5-3[c]	Cyclo(Ala–Ala)	1	—	2.5	25	28	75	3000	2500	1.27
P5-4[c]	Cyclo(Ala–Ala)	1	—	2.75	25	21	75	3000	3000	1.27
P5-5[c]	Cyclo(Gly–Gly)	1	—	2.75	25	21	75	3000	3100	1.28

[a] Reactant equivalents compared to 1 equivalent of DKP. [b] THF was used as the polymerization solvent. [c] MeTHF was used as the polymerization solvent.

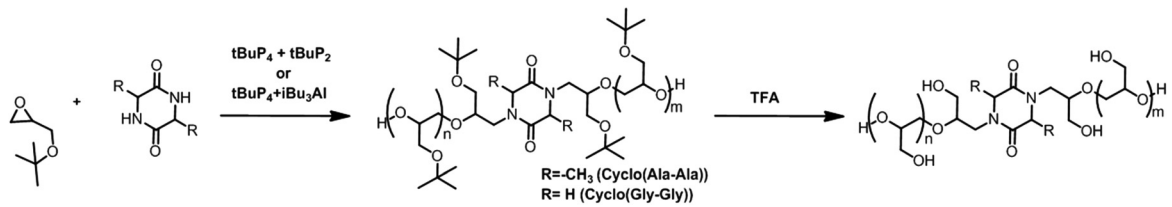

Scheme 2 Synthesis of *N*-P*t*BuGE-DKP and *N*-PG-DKP.

expected structures (Fig. S20 and S21†). The synthesis of *N*-P*t*BuGE-DKPs with $tBuP_4$/i-Bu_3Al yielded slightly broad dispersities compared to the $tBuP_2$/$tBuP_4$ system; however, the control over the molar mass was more efficient, and the obtained M_n values by GPC were exactly matching with the targeted ones. Finally, P5-4 was deprotected by trifluoro acetic acid according to Erberich *et al.*[48] and purified by dialysis against distilled water to yield the water soluble *N*-polyglycerol-Cyclo(Ala–Ala) (*N*-PG-Cyclo(Ala–Ala)) (Fig. S23†) which could provide new opportunities for biological applications.

Conclusions

We have successfully synthesized a library of well-defined *N*-polyether-DKPs *via* AROP. Mild polymerization conditions have been identified allowing the elimination of the side-reactions, which occurred only when $tBuP_4$ phosphazene base was used. *N*-Polyether-DKPs were carefully characterized using GPC, MALDI-ToF, ATR-FTIR, and ^{1}H- and ^{13}C-NMR. Epimerization reactions were eliminated by the addition of i-Bu_3Al in the reaction medium, leading to the preparation of mono-isomeric *N*-substituted DKPs with nevertheless slightly broader dispersities. Linear polyglycidol and poly(butylene oxide) chains were substituted demonstrating the possibility of the creation of both hydrophilic and hydrophobic substituents and the development of novel materials through self-assembly for biomedical applications (Scheme 2).

Experimental

Materials

All the DKPs, Cyclo(alanine–alanine) (Aldrich), Cyclo(glycine–glycine) (Aldrich), Cyclo(Val–Val) (Bachem) and Cyclo(phenylalanine–phenylalanine) (Bachem), phosphazene base $tBuP_4$ solution (0.8 mol L^{-1} in hexane, Aldrich), phosphazene base $tBuP_2$ solution (2 mol L^{-1} in THF, Aldrich), 2-methyltetrahydrofuran (MeTHF) (98%, Aldrich), and tri-isobutyl aluminum (i-Bu_3Al) solution (1.0 mol L^{-1} in hexane, Aldrich) were used without further purification. 1,2-Epoxybutane (99%, Aldrich) and *t*-butyl glycidyl ether (99%, Aldrich) were distilled over CaH_2 two times prior to use. Tetrahydrofuran was dried with an MBRAUN MB SPS-800 solvent purification system under nitrogen.

Instrumentation

^{1}H and ^{13}C NMR analyses were performed on Bruker Avance 300 MHz and Bruker Avance 400 MHz spectrometers. All spectra were internally referenced to the residual proton signals of the deuterated solvent: $CDCl_3$ and THF-d8. Polymer molar masses were determined by size exclusion chromatography (SEC) with three PLGel Mixte C 5 μm columns (7.5 × 300 mm; separation limits: 0.2 to 2000 kg mol^{-1}) maintained at 40 °C coupled with 2 modular detectors: a differential refractive index (RI) detector Viscotek 3580 and a diode array UV detector Shimadzu SPD20-AV. THF was used as the mobile phase at a flow rate of 1 mL min^{-1}, and toluene was used as a flow rate marker. All polymers were injected (100 μL) at a concentration of 5 mg mL^{-1} after filtration through a 0.45 μm pore-size membrane. OmniSEC 4.7 software was used for data acquisition and data analysis. The number-average molar masses ($\bar{M}_n$), the weight-average molar masses ($\bar{M}_w$), and the molar mass distributions ($Đ = \bar{M}_w/\bar{M}_n$) were determined by SEC with a calibration curve based on narrow poly(methyl methacrylate) (PMMA) standards (from Polymer Standard Services), using the RI detector.

MALDI-ToF. Mass spectra were recorded by matrix-assisted laser desorption and ionization time-of-flight (MALDI-ToF)

mass spectrometry (MS) using a Bruker autoflex III smartbeam mass spectrometer, equipped with a laser that produces pulses at 337 nm using dithranol as a matrix and NaI as a cationizing agent. Spectra were recorded in reflectron or in linear mode at an accelerating potential of 20 kV. Samples were prepared by dissolving the polymer in THF at a concentration of 5 mg mL^{-1}. A 10 μL aliquot of this solution was mixed with 20 μL of dithranol solution as the matrix (at 20 mg mL^{-1} in THF) and 10 μL of NaI solution (at 10 mg mL^{-1} in THF). Standards (poly (ethylene oxide) of known structures, $\bar{M}_n$ = 1470 and 4250 g mol^{-1} purchased from Polymer Standards Service) were used to calibrate the mass scale.

FTIR experiments. FTIR spectra in the attenuated total reflection (ATR) mode were recorded on a Bruker Equinox 55 spectrometer using a spectral resolution of 4 cm^{-1}. The spectrometer was continuously purged with dry air to avoid water vapor absorption in the spectral range of amide and ester carbonyl absorptions. 60 μL of the polymer solution in CH_2Cl_2 was deposited on the bare ATR element made of germanium allowing 15 useful internal reflections and the solvent was allowed to evaporate before collecting 128 scans. Each recorded spectrum was transformed by ATR correction to the absorption spectrum.

Polymerization conditions for Tables 1–3, P5-1 and P5-2, Table 5

The polymerization was carried out according to the following typical procedure. The initiator precursor DKP was weighed into a reaction flask. Then, the rest of the reactant was added to a glove-box. Following the initiator, the solvent (THF) was added to the reactor. Then *t*-BuP_4 and *t*-BuP_2 were added. Finally the monomer, 1,2-epoxybutane, was added and the reactor was closed with a septum. After the closure of the reaction flask, the reaction mixture was stirred at room temperature or at 40 °C and left to react for the required period of time. A small portion of the reaction mixture was sampled through a septum at various reaction times for NMR analyses. The reaction was quenched by addition of 0.1 mL of 1% acetic acid. The polymer was dissolved in ethyl acetate and purified by passing through neutralized aluminum oxide, filtering, and removing the solvent under vacuum at 50 °C to give a colorless viscous liquid.

Polymerization conditions for Tables 4 and 5 (P5-3, P5-4 and P5-5)

The polymerization was carried out according to the following typical procedure. The initiator precursor DKP was weighed into a reaction flask. Then, the rest of the reactant was added to a glove-box. After the initiator, the solvent (MeTHF) was added to the reactor. Then *t*-BuP_4 was added. Subsequently, i-Bu_3Al was added and stirred until the complete dissolution of DKP (2 h to 4 h). Finally, the monomer 1,2-epoxybutane was added using a microsyringe. The reaction mixture was stirred at the indicated temperature and left to react for the required period of time. A small portion of the reaction mixture was sampled through a septum at various reaction times for NMR analyses. The reaction was quenched by the addition of 0.1 mL of 1% acetic acid in H_2O. The polymer was dissolved in ethyl acetate and purified by passing through neutralized aluminum oxide, filtering, and removing the solvent under vacuum at 50 °C to give a colorless viscous liquid.

Conflicts of interest

There are no conflicts to declare.

Acknowledgements

This work was supported by the Sorbonne Universités Emergence 2016 program of the French state funds managed by the ANR within the Investisements D'Avenir programme under reference number ANR-11-IDEX-0004-02 and funding from the French National Funding Agency (ANR-17-CE18-0015-01 - VINP).

References

1 H. Habashita, M. Kokubo, S.-i. Hamano, N. Hamanaka, M. Toda, S. Shibayama, H. Tada, K. Sagawa, D. Fukushima, K. Maeda and H. Mitsuya, *J. Med. Chem.*, 2006, **49**, 4140–4152.
2 V. Mas, A. Falco, I. Brocal, L. Perez, J. M. Coll and A. Estepa, *Antiviral Res.*, 2006, **72**, 107–115.
3 K.-H. Rhee, *Int. J. Antimicrob. Agents*, 2004, **24**, 423–427.
4 M. P. d. Carvalho and W. R. Abraham, *Curr. Med. Chem.*, 2012, **19**, 3564–3577.
5 K. Kanoh, S. Kohno, J. Katada, Y. Hayashi, M. Muramatsu and I. Uno, *Biosci., Biotechnol., Biochem.*, 1999, **63**, 1130–1133.
6 A. K. Szardenings, D. Harris, S. Lam, L. Shi, D. Tien, Y. Wang, D. V. Patel, M. Navre and D. A. Campbell, *J. Med. Chem.*, 1998, **41**, 2194–2200.
7 S. R. Naini, R. A. Lalancette, O. Gorlova, K. V. S. Ramakrishna, J. S. Yadav and S. Ranganathan, *Eur. J. Org. Chem.*, 2014, **2014**, 7015–7022.
8 K. B. Joshi and S. Verma, *Tetrahedron Lett.*, 2008, **49**, 4231–4234.
9 M. J. Seo, J. Song, C. Kantha, M. I. Khazi, U. Kundapur, J.-M. Heo and J.-M. Kim, *Langmuir*, 2018, **34**, 8365–8373.
10 Z. Xie, A. Zhang, L. Ye, X. Wang and Z.-g. Feng, *J. Mater. Chem.*, 2009, **19**, 6100–6102.
11 S. Manchineella, N. A. Murugan and T. Govindaraju, *Biomacromolecules*, 2017, **18**, 3581–3590.
12 A. Jeziorna, K. Stopczyk, E. Skorupska, K. Luberda-Durnas, M. Oszajca, W. Lasocha, M. Górecki, J. Frelek and M. J. Potrzebowski, *Cryst. Growth Des.*, 2015, **15**, 5138–5148.
13 J. W. Loergen, C. Kreutz, J. Bargon, P. Krattiger and H. Wennemers, *Sens. Actuators, B*, 2005, **107**, 366–371.

14 Q. Zhao and C. E. Schafmeister, in *Peptidomimetics II*, ed. W. Lubell, Springer International Publishing, Cham, 2017, pp. 51–80, DOI: 10.1007/7081_2015_165.

15 O. Ovadia, S. Greenberg, J. Chatterjee, B. Laufer, F. Opperer, H. Kessler, C. Gilon and A. Hoffman, *Mol. Pharm.*, 2011, **8**, 479–487.

16 E. Biron, J. Chatterjee, O. Ovadia, D. Langenegger, J. Brueggen, D. Hoyer, H. A. Schmid, R. Jelinek, C. Gilon, A. Hoffman and H. Kessler, *Angew. Chem., Int. Ed.*, 2008, **47**, 2595–2599.

17 C. K. Wang, S. E. Northfield, B. Colless, S. Chaousis, I. Hamernig, R.-J. Lohman, D. S. Nielsen, C. I. Schroeder, S. Liras, D. A. Price, D. P. Fairlie and D. J. Craik, *Proc. Natl. Acad. Sci. U. S. A.*, 2014, **111**, 17504–17509.

18 P. A. Wender, D. J. Mitchell, K. Pattabiraman, E. T. Pelkey, L. Steinman and J. B. Rothbard, *Proc. Natl. Acad. Sci. U. S. A.*, 2000, **97**, 13003–13008.

19 Y.-U. Kwon and T. Kodadek, *J. Am. Chem. Soc.*, 2007, **129**, 1508–1509.

20 N. P. Chongsiriwatana, J. A. Patch, A. M. Czyzewski, M. T. Dohm, A. Ivankin, D. Gidalevitz, R. N. Zuckermann and A. E. Barron, *Proc. Natl. Acad. Sci. U. S. A.*, 2008, **105**, 2794–2799.

21 N. P. Chongsiriwatana, T. M. Miller, M. Wetzler, S. Vakulenko, A. J. Karlsson, S. P. Palecek, S. Mobashery and A. E. Barron, *Antimicrob. Agents Chemother.*, 2011, **55**, 417–420.

22 J. G. Beck, J. Chatterjee, B. Laufer, M. U. Kiran, A. O. Frank, S. Neubauer, O. Ovadia, S. Greenberg, C. Gilon, A. Hoffman and H. Kessler, *J. Am. Chem. Soc.*, 2012, **134**, 12125–12133.

23 J. Chatterjee, C. Gilon, A. Hoffman and H. Kessler, *Acc. Chem. Res.*, 2008, **41**, 1331–1342.

24 J. F. Reichwein and R. M. J. Liskamp, *Tetrahedron Lett.*, 1998, **39**, 1243–1246.

25 D. T. S. Rijkers, J. W. M. Höppener, G. Posthuma, C. J. M. Lips and R. M. J. Liskamp, *Chem. – Eur. J.*, 2002, **8**, 4285–4291.

26 J. Ying, X. Gu, M. Cai, M. Dedek, J. Vagner, D. B. Trivedi and V. J. Hruby, *J. Med. Chem.*, 2006, **49**, 6888–6896.

27 A. I. Fernández-Llamazares, J. García, V. Soto-Cerrato, R. Pérez-Tomás, J. Spengler and F. Albericio, *Chem. Commun.*, 2013, **49**, 6430–6432.

28 A. I. Fernández-Llamazares, J. Adan, F. Mitjans, J. Spengler and F. Albericio, *Bioconjugate Chem.*, 2014, **25**, 11–17.

29 A.-C. Albertsson and I. K. Varma, *Biomacromolecules*, 2003, **4**, 1466–1486.

30 A. Thomas, S. S. Müller and H. Frey, *Biomacromolecules*, 2014, **15**, 1935–1954.

31 N. Badi, L. Auvray and P. Guegan, *Adv. Mater.*, 2009, **21**, 4054–4057.

32 S. Boileau and N. Illy, *Prog. Polym. Sci.*, 2011, **36**, 1132–1151.

33 J. Zhao, N. Hadjichristidis and Y. Gnanou, *Polimery*, 2014, **59**, 49–59.

34 L. Hassouna, N. Illy and P. Guégan, *Polym. Chem.*, 2017, **8**, 4005–4013.

35 L. Dentzer, C. Bray, S. Noinville, N. Illy and P. Guegan, *Macromolecules*, 2015, **48**, 7755–7764.

36 M. Shivaprasad and G. T. Govindaraju, *ChemPlusChem*, 2017, **82**, 88–106.

37 L. Raguine, M. Ali, V. Bender, E. Diefenbach, M. R. Doddareddy, D. Hibbs and N. Manolios, *Chem. Biol. Drug Des.*, 2013, **81**, 167–174.

38 H. Misaka, E. Tamura, K. Makiguchi, K. Kamoshida, R. Sakai, T. Satoh and T. Kakuchi, *J. Polym. Sci., Part A: Polym. Chem.*, 2012, **50**, 1941–1952.

39 S. L. Malhotra, A. Leborgne and L.-P. Blanchard, *J. Polym. Sci., Polym. Chem. Ed.*, 1978, **16**, 561–582.

40 S. L. Portnova, V. F. Bystrov, T. A. Balashova, V. T. Ivanov and Y. A. Ovchinnikov, *Bull. Acad. Sci. USSR, Div. Chem. Sci.*, 1970, **19**, 776–780.

41 C. Eguchi and A. Kakuta, *J. Am. Chem. Soc.*, 1974, **96**, 3985–3989.

42 T. Munegumi, T. Fujimoto, M. Takada and N. Nagashima, *Orient. J. Chem.*, 2014, **1**, 23–30.

43 A. S. Culf, M. Čuperlović-Culf, D. A. Léger and A. Decken, *Org. Lett.*, 2014, **16**, 2780–2783.

44 C. Caumes, C. Fernandes, O. Roy, T. Hjelmgaard, E. Wenger, C. Didierjean, C. Taillefumier and S. Faure, *Org. Lett.*, 2013, **15**, 3626–3629.

45 V. M. Tul'chinskii, A. I. Miroshnikov, P. V. Kostetskii and G. A. Kogan, *Chem. Nat. Compd.*, 1973, **9**, 745–751.

46 A. Shoji, T. Ozaki, H. Saitô, R. Tabeta and I. Ando, *Die Makromol. Chem. Rapid Commun.*, 1984, **5**, 799–804.

47 C. Billouard, S. Carlotti, P. Desbois and A. Deffieux, *Macromolecules*, 2004, **37**, 4038–4043.

48 M. Erberich, H. Keul and M. Möller, *Macromolecules*, 2007, **40**, 3070–3079.